**Electronic Supplementary Information (ESI)**

# Mapping Protein-Specific Micro-Environments in Live Cells by Fluorescence Lifetime Imaging of a Hybrid Genetic-Chemical Molecular Rotor Tag

**Evangelos Gatzogiannis[†a,b], Zhixing Chen[†a], Lu Wei[a], Richard Wombacher[a,c], Ya-Ting Kao[a], Grygorii Yefremov[a], Virginia W. Cornish[a], Wei Min[a]**

[a] *Department of Chemistry, Columbia University, New York, NY 10027*

[b]Current Address: *National Institute of Standards and Technology, Gaithersburg, MD, 20899*

[c]Current Address: *Institute of Pharmacy and Molecular Biotechnology, Heidelberg University, Heidelberg D-69210, Germany*

†These two authors are equal main contributors

*E-mail: wm2256@columbia.edu

**Content**



## 1. Synthesis and characterization of TMP-Cy3

Anhydrous dimethylformamide was obtained from Aldrich, triethylamine was obtained from Fluka. TMP-PEG-$NH_2$ (TFA salt) was reported previously[1]. Cy3 NHS ester was obtained from Lumiprobe, LLC. Nuclear magnetic resonance (NMR) spectra were recorded on a Bruker 400 (400MHz) Fourier Transform (FT) NMR spectrometer at the Columbia University Chemistry Department. 1H NMR spectra are tabulated in the following order: multiplicity (s, singlet; d, doublet; t, triplet; m, multiplet). Electron spray ionization (ESI) MS were recorded on a JMS-LC Mate mass spectrometer.

***TMP-Cy3***

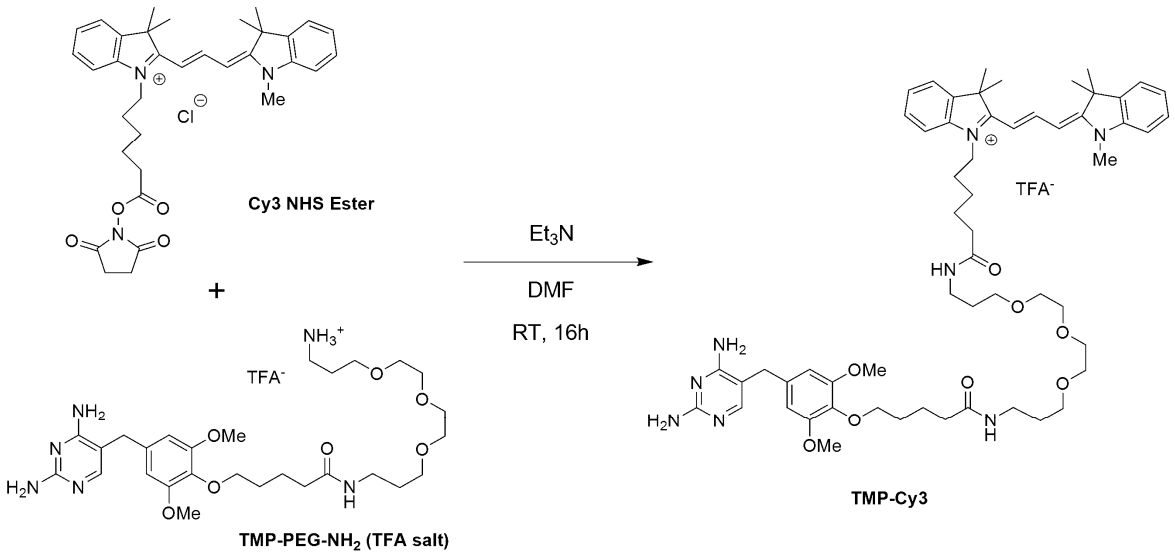


**Scheme S1. Synthesis of TMP-Cy3**

In a 5.0 mL vial TMP-PEG-$NH_2$ (TFA salt) (1.0 mg, 1.4 μmol) and Cy3 NHS-ester (1.2 mg, 2.0 μmol) were dissolved in 0.2 mL of anhydrous dimethylformamide (DMF). Triethylamine (TEA) (5.0 μL, 50.0 μmol) was added to the vial and the reaction was stirred overnight at low light and at room temperature. The reaction mixture was concentrated to dryness, re-dissolved in 3.0 mL of $H_2O$/$CH_3CN$ 4:1 (v/v) and purified by preparative HPLC using a linear gradient of solvent $H_2O$ (0.1% TFA) / $CH_3CN$ 80 / 20 to 40 / 60 over 40 min to give 1.6 mg TMP-Cy3 as a pink-brown solid (near quantitative) with a retention time of 24.6 min.

**$^1$H NMR** (400 MHz, MeOD) δ ppm: 8.55 (t, *J* = 13.6 Hz, 1 H); 7.55 (d, *J* = 7.2 Hz, 2 H); 7.45 (m, 2 H); 7.37-7.29 (m, 4 H); 7.22 (s, 1 H); 6.56 (s, 2 H); 6.45 (d, *J* = 13.6 Hz, 1 H); 6.43 (d, *J* = 13.6 Hz, 1 H); 4.15 (t, *J* = 7.0 Hz, 2 H); 3.91 (t, *J* = 6.2 Hz, 2 H); 3.79 (s, 6 H); 3.69 (s, 3 H); 3.66 (s, 2 H); 3.62-3.60 (m, 4 H); 3.57-3.54 (m, 4 H); 3.50 (t, *J* = 6.2 Hz, 2 H); 3.47 (t, *J* = 6.4 Hz, 2 H); 3.25 (t, *J* = 6.8 Hz, 2 H); 3.22 (t, *J* = 6.8 Hz, 2 H); 2.25 (t, *J* = 7.2 Hz, 2 H); 2.21 (t, *J* = 7.2 Hz, 2 H); 1.88-1.68 (m, 12 H); 1.77 (s, 12 H); 1.48 (m, 2 H). MS (ESI+) m/z Calcd for $C_{58}H_{81}O_8N_8^+$ $[M]^+$: 1017.62, Found: 1017.93

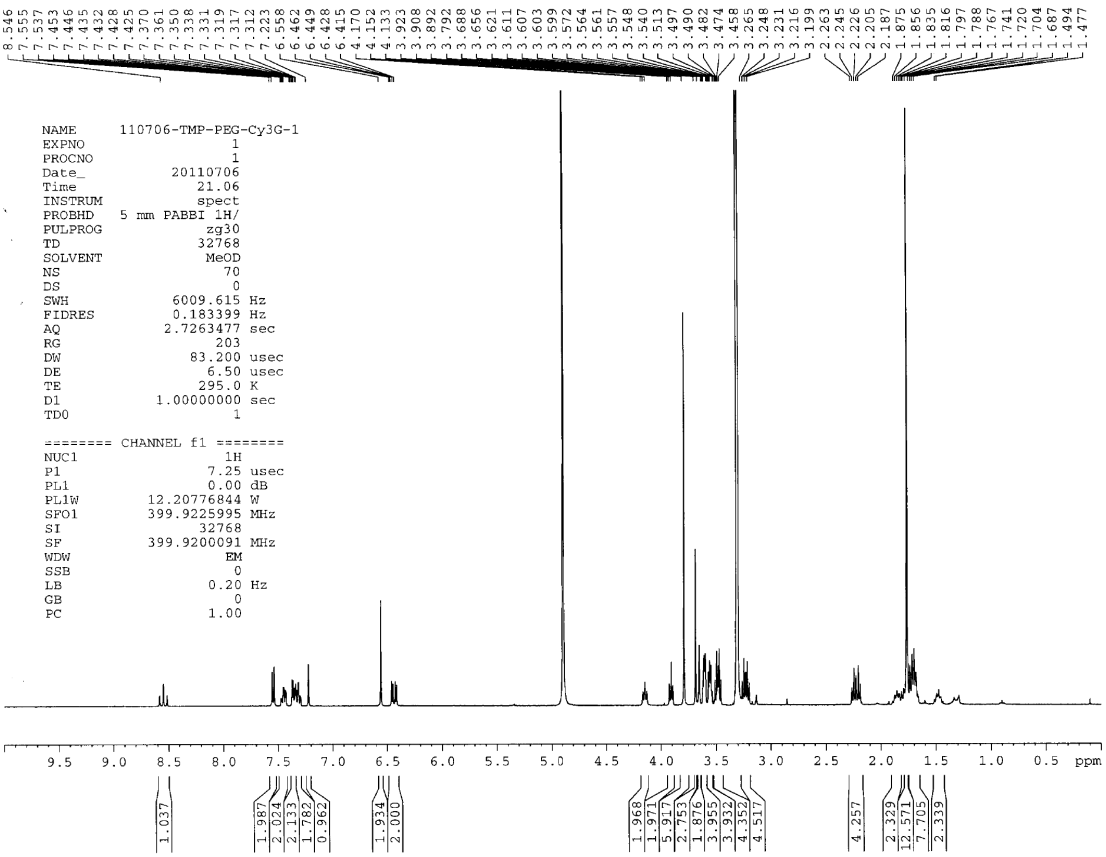
NAME 110706-TMP-PEG-Cy3G-1
EXPNO 1
PROCNO 1
Date_ 20110706
Time 21.06
INSTRUM spect
PROBHD 5 mm PABBI 1H/
PULPROG zg30
TD 32768
SOLVENT MeOD
NS 70
DS 0
SWH 6009.615 Hz
FIDRES 0.183399 Hz
AQ 2.7263477 sec
RG 203
DW 83.200 usec
DE 6.50 usec
TE 295.0 K
D1 1.00000000 sec
TD0 1
======== CHANNEL f1 ========
NUC1 1H
P1 7.25 usec
PL1 0.00 dB
PL1W 12.20776844 W
SFO1 399.9225995 MHz
SI 32768
SF 399.9200091 MHz
WDW EM
SSB 0
LB 0.20 Hz
GB 0
PC 1.00
ppm

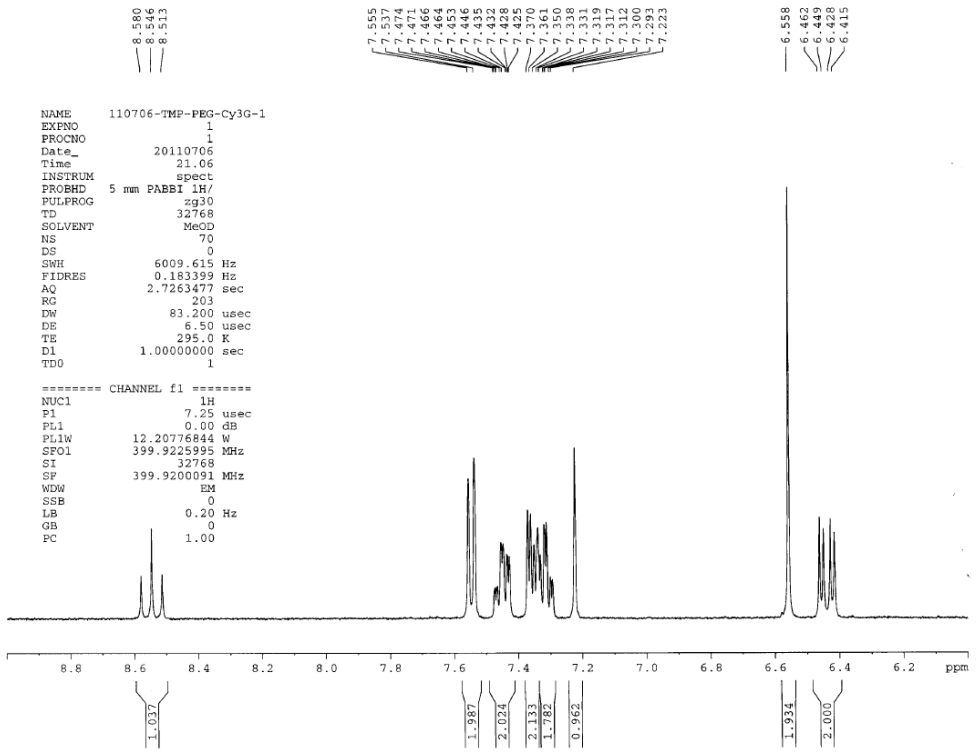
NAME 110706-TMP-PEG-Cy3G-1
EXPNO 1
PROCNO 1
Date_ 20110706
Time 21.06
INSTRUM spect
PROBHD 5 mm PABBI 1H/
PULPROG zg30
TD 32768
SOLVENT MeOD
NS 70
DS 0
SWH 6009.615 Hz
FIDRES 0.183399 Hz
AQ 2.7263477 sec
RG 203
DW 83.200 usec
DE 6.50 usec
TE 295.0 K
D1 1.00000000 sec
TD0 1
======== CHANNEL f1 ========
NUC1 1H
P1 7.25 usec
PL1 0.00 dB
PL1W 12.20776844 W
SFO1 399.9225995 MHz
SI 32768
SF 399.9200091 MHz
WDW EM
SSB 0
LB 0.20 Hz
GB 0
PC 1.00
ppm

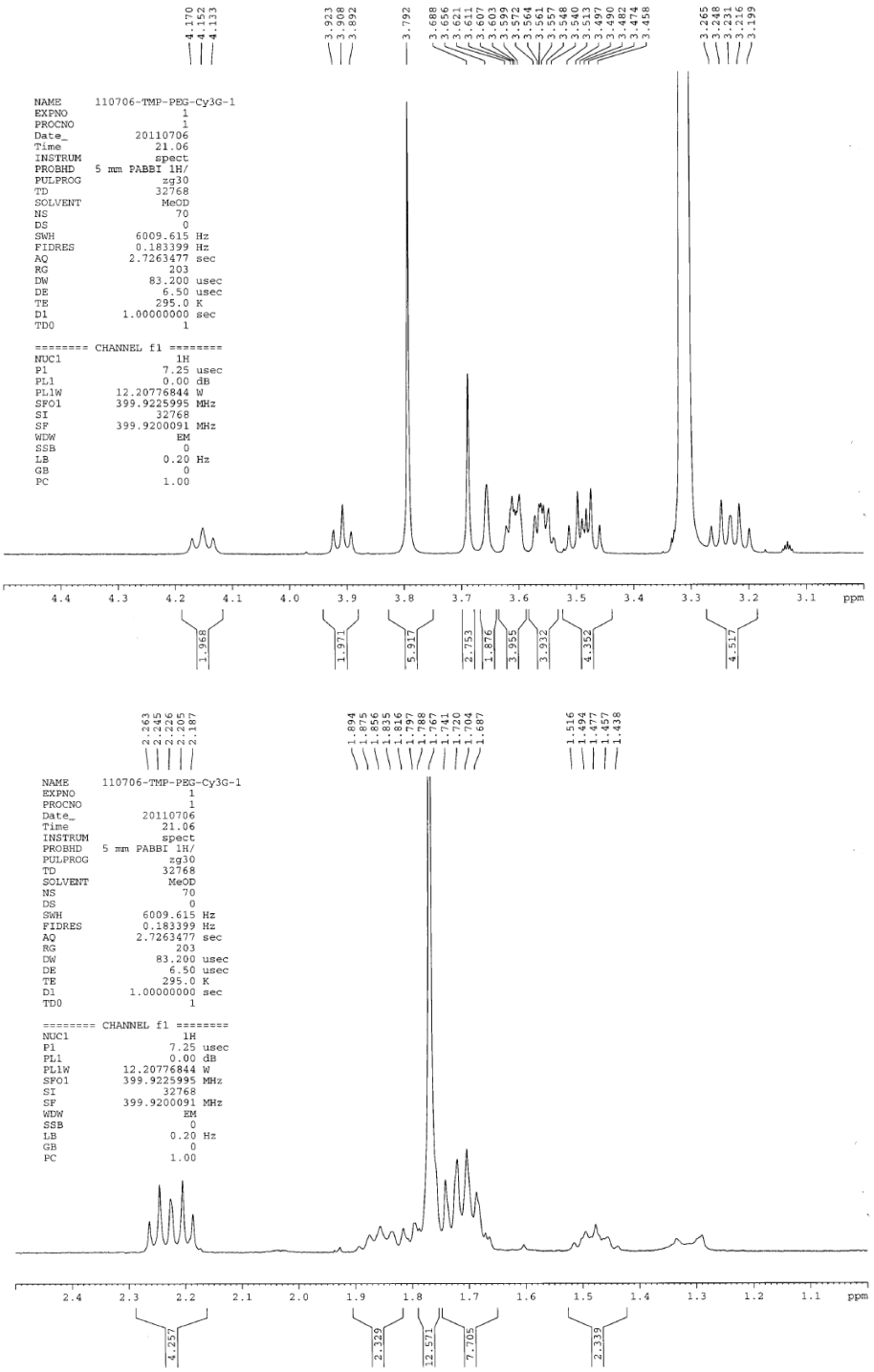


**Figure S1.[1]HNMR spectra of TMP-Cy3 (MeOD, 400 MHz), including H shift and multi-splitting.**

## 2. Experimental Procedures

### Cell culture, transfection and labeling

HEK 293T cells were cultured in DMEM w/ glutamine (Gibco #11995) with 10% v/v fetal bovine serum and 1% v/v Pen./Strep. Cells were maintained under 5% $CO_2$ at 37°C. For *in vivo* labelling, cells were plated in eight-well chambered #1 borosilicate coverglass-bottomed chambers (Thermo, Nunc 155411) twenty-four hours before transfection with expression plasmids for H2B-eDHFR[2]or PMLS-eDHFR[3] (0.4 μg DNA for one well) using Fugene HD (Roche). Twenty four hours after transfection, 300 μL of cell culture media was added and 0.24 μL TMP-Cy3 stock solution (1.25 mM in DMF) for a final TMP-Cy3 concentration of 1 μM. Cells were incubated with this staining solution for 10 min at 37°C, and then washed twice with fresh media before imaging at room temperature (25°C). All spectroscopy and imaging experiments were performed at room temperature.

### Fluorescence Imaging

Imaging was performed using a home-built confocal microscope configured on an inverted microscope body (IX71, Olympus) and operated in a sample scanning mode. A 532 nm diode laser (Compass 215M, Coherent) was used to excite the Cy3-labeled cells. A number of confocal fluorescence images were also captured on a commercial confocal laser scanning microscope (SP5, Leica) with the 488 and 514 nm lines of the Argon Ion laser for Fluoroscein and Cy3, respectively, and a 594nm laser line for mCherry imaging. All measurements were performed at room temperature.

Untransfected cells (Figure S2, top row) display minor degrees of background staining but no localization of TMP-Cy3 to the nuclei as in the middle row of Figure S2, where TMP-Cy3 rapidly localizes to H2B-eDHFR in the nucleus of H2B-eDHFR transfected 293T cells. The nuclei are quite dark in the first row of Figure S2, compared to the row below, where TMPCy3 targeted H2B-eDHFR labeled protein within the nuclei.

Several tests were performed to assess whether H2B-eDHFR-TMP-Cy3 fusion protein distributes the same as native H2B protein. Cells were also transfected to express H2B-mCherry, mCherry is a bright red fluorescent protein that provides direct imaging of H2B in live cells. We imaged H2B-mCherry transfected cells simultaneously with H2B-eDHFR transfected cells in order to verify that eDHFR does indeed target H2B protein with high specificity in live cells. Cells were co-labeled with H2B-eDHFR-TMP-Cy3 and H2B-mCherry and the degree of overlap was assessed (Figure S2). There is good overlap between H2B-eDHFR-TMP-Cy3 staining and H2B-mCherry images at the bottom right of Figure S2. Confocal fluorescence images are overlaid with DIC in the last column to the right. From left to right all images present confocal fluorescence from Cy3, mCherry, the DIC image and the overlay of fluorescence with DIC. In Figure S2A the two images outlined in red, of transfected H2B-eDHFR-TMP-Cy3 and its corresponding DIC image are expanded to help demonstrate the localization of TMP-Cy3 to the nucleus and the observed background staining. In Figure S3 the last row of Figure S2 is blown up to further reveal the DIC contrast and overlaid images in order to provide a sense of the original 512x512 pixel resolution images that is not provided in Figure S2.

In order to address the non-specific staining of TMP-Cy3 to mitochondria and potentially other cellular organelles, we imaged 293T cells transfected with H2B-eDHFR and then stained with TMP-Fluorescein, Figure S4. In this control image we observe that eDHFR is well targeted to cell nuclei and doesn't perturb cell functions such as chromatin formation. In addition TMP-Fluorescein did not exhibit the background staining that Cy3 has shown, for example in Figure 2, where H2B-TMP-Cy3 exhibits a markedly higher level of background staining compared to H2B-mCherry. However, Cy3 does exhibit viscosity sensitivity, unlike Fluorescein. Efforts are underway towards developing a better-behaved molecular rotor, and other environmental probes.

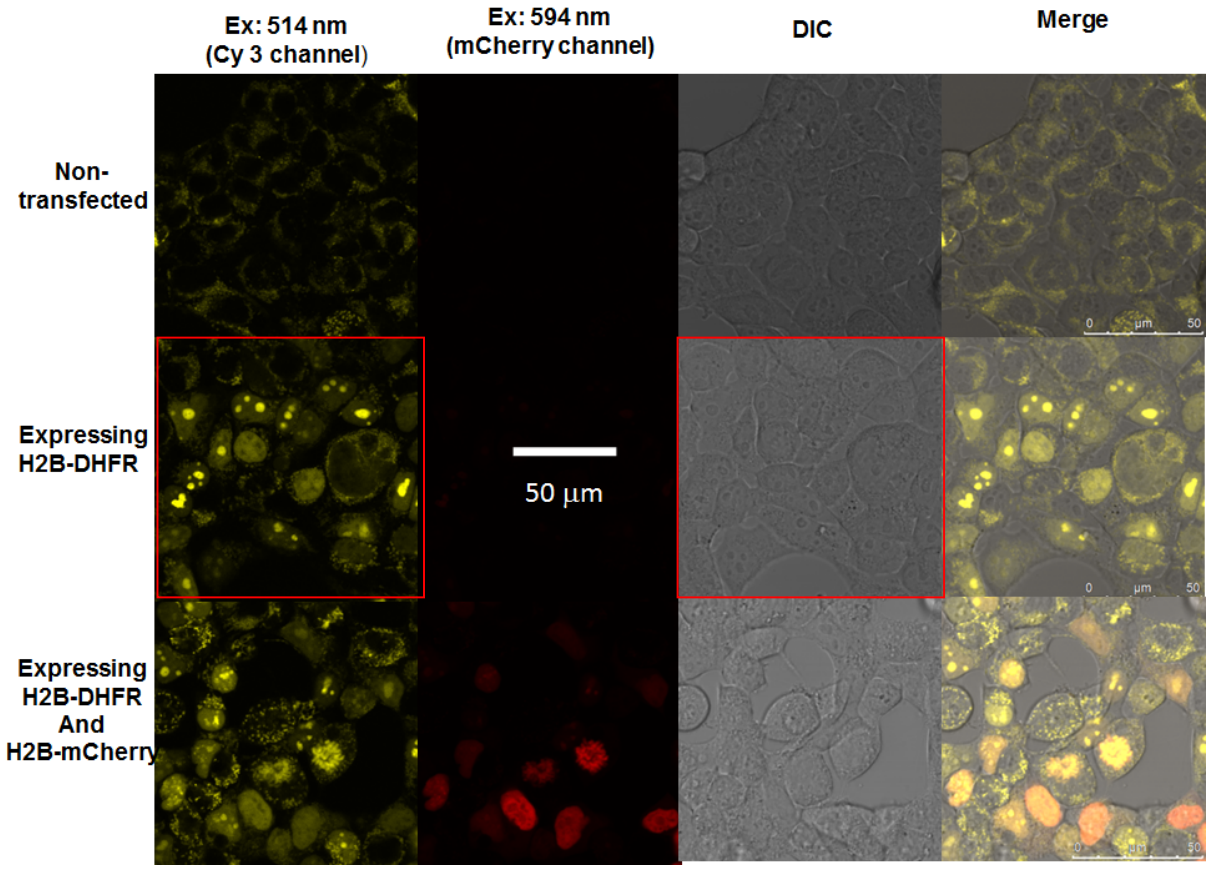


**Figure S2. Confocal fluorescence of untransfected (top row), H2B-eDHFR transfected (middle row) and H2B-eDHFR and H2B-mCherry dual transfected cells (bottom row). Fluorescence was monitored from left to right with 514nm excitation for Cy3 and 594nm excitation for H2B-mCherry, the DIC image is provided in the third column and the overlay of the Cy3, mCherry fluorescence and DIC is shown in the last column.**

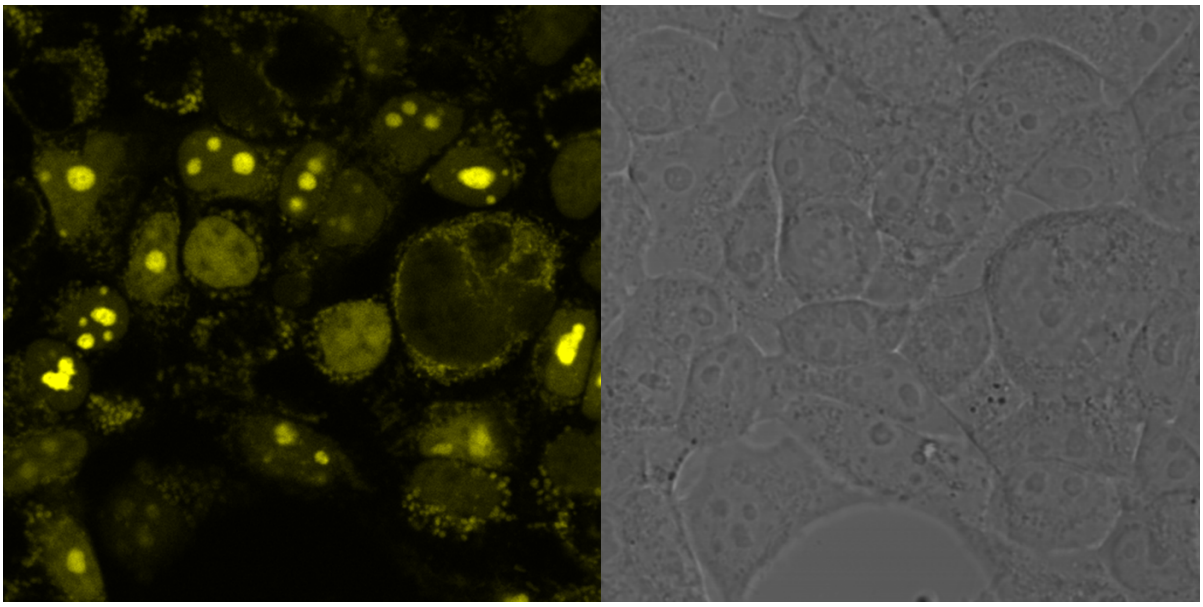

**Figure S2A. H2B-eDHFR-TMP-Cy3 fluorescence image and its corresponding DIC image revealing cell outlines and nuclei/nucleoli.**

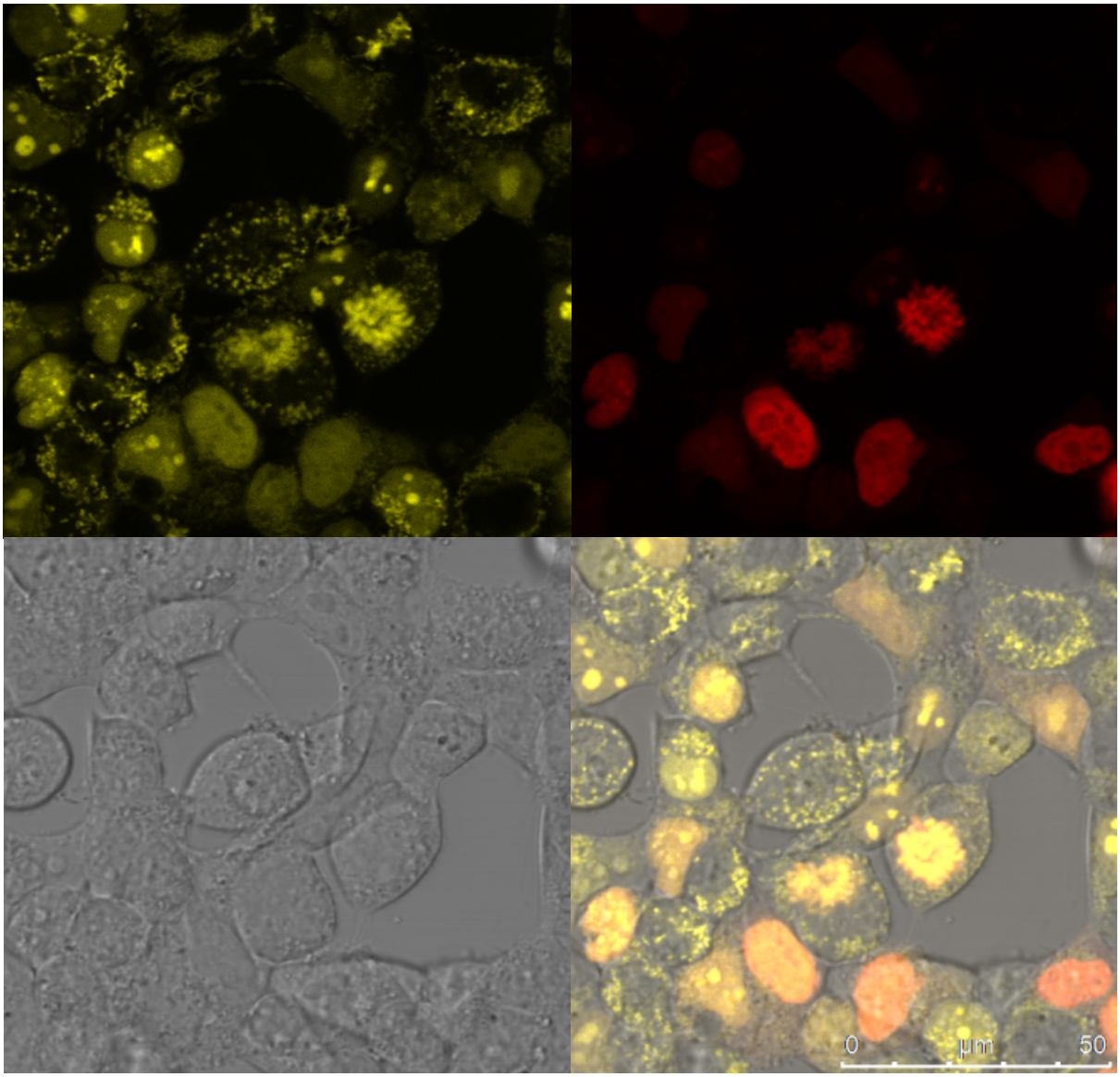


**Figure S3. The bottom row of Figure S2 is expanded, illustrating H2B-eDHFR-TMP-Cy3 fluorescence (top left), H2B-mCherry fluorescence (top right), DIC (bottom left), and the overlay of all three images (bottom right).**

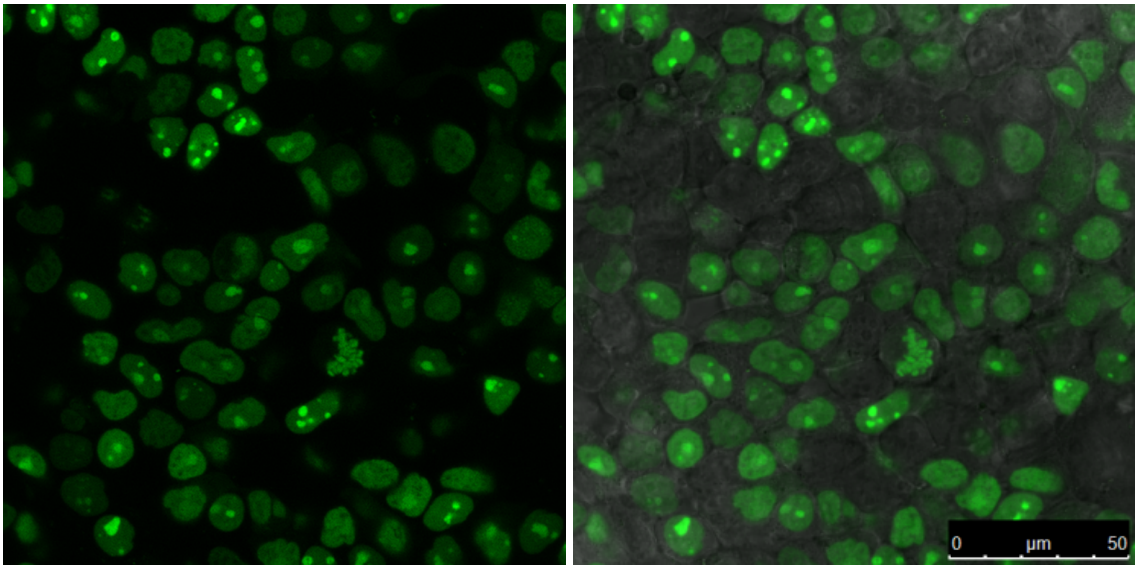


**Figure S4. Confocal fluorescence of 293T cells transfected with H2B-eDHFR and labeled with Fluorescein. Cells were excited with a 488nm laser line and confocal fluorescence images were acquired. Scale bar 50** µm.

## Fluorescence lifetime imaging microscopy (FLIM)

A home-built FLIM microscope capability was configured by modulating the 532nm excitation laser at 50MHz with an acousto-optic modulator (3200-121, Crystal Technology) driven by a sine wave from an arbitrary function generator (AFG 3102, Tektronix). The 532 nm beam was focused by a 50mm achromatic lens into the AOM, which was centered in a 4X beam expanding telescope. The undiffracted zeroth order beam was selected. A dichroic filter (Di01-R532-25x35, Semrock) directed the sinusoidally-modulated excitation laser onto the sample and the same objective was used to collect the sinusoidally-modulated and phase-shifted fluorescence. A high-NA water lens (60x 1.2NA UPLANSAPO, Olympus) was used for all FLIM images. A Hamamatsu R9110 photomultiplier tube (PMT) was placed at the microscope side port primary image plane, with a 50 µm pinhole serving as the confocal pinhole. After passing through the microscope internal optics and a long-pass filter, the fluorescence was detected by the PMT. The PMT electrical signal was pre-amplified by a wide-bandwidth (up to 50 MHz) pre-amplifier (C6438-01, Hamamatsu) and input directly into a dual-phase RF lock-in amplifier (SR844, Stanford Research Systems).

A frequency-domain fluorescence lifetime approach was used with sinusoidal modulation at 50 MHz and subsequent de-modulation and extraction of the phase lag using a dual-phase wide bandwidth lock-in amplifier. Both the in-phase **(X)** and out-of-phase component **(Y)** of the sinusoidally-modulated fluorescence, relative to the excitation sine wave, are determined by the lock-in amplifier and the phase difference (lag) is computed and defined as:

$$\theta \equiv \arctan(Y/X) \qquad \textbf{(Equation S1)}$$

The phase lag was measured for each pixel and recorded using home-written software in LabView that also moved the nanometric sample-scanning stage. Pixel dwell times from 100 µs to 3ms were used. Pixel dwell times were set equal to the lock-in time constant. A lock-in time constant of 1 ms gave the best results (26 seconds per frame at 100x100 pixels), and a 300 µs time constant provided satisfactory imaging at a significantly faster rate (6s per frame). For imaging, depending on the specific protein that was transfected either 3 volts were sent to the nanometric sample scanning stage, which defined a total scan area of 21µm x 21µm (typically used for the nuclear H2B protein images) or 9-10 Volts for a total scan area of 63-70µm x 63-70 µm (typically used for the PMLS plasma membrane protein images). 100x100 or 200x200 pixels defined the imaging area for most images, with each pixel corresponding to 210 nm or 315 nm, both below or comparable to the diffraction limit of the objective lens used.

A modulation frequency of 50MHz was used for frequency domain fluorescence lifetime measurements. This frequency was chosen because a) it is sufficient for frequency-domain phase fluorometry (~20ns per period) and b) it is an upper limit of performance for our AOM. At modulator driving frequencies above 50MHz there is a substantial decrease in modulation depth and a distortion of the laser output. Modulation depth and AOM stability are key parameters for the quality of the lifetime imaging. Several control experiments revealed that the phase shift of Cy3 in various glycerol mixtures was always between that of the laser response and Rhodamine 6G, Rhodamine 6G displaying the largest phase lag (most negative phase), Cy3 an intermediate lag, and the laser response always the most positive of the three. The phase of the sinusoidally-modulated fluorescence was compared to that of the excitation laser for all measurements. To determine the instrument response, the long-pass filter was removed from its position right before the confocal pinhole and an image was taken of the modulated laser reflection from the glass coverslip surface, a mirrored microscope slide, or by focusing on the bottom of the 8 well coverglass-bottomed chambered cell slide. Care must be taken with this approach, as the focus may alter the phase shift. Focusing into a solution of a well-known dye like Rhodamine6G is more appropriate in some cases, as the distribution of phases is narrower and the solution presumably where the cells would be (minimizing optical phase shifts). The reflection image serves as a measurement of all the delays due to system electronics and optics. The reflected laser image is then averaged to give an instrumental phase. This instrumental phase must be subtracted from the total phase of the sample and instrument in order to determine the sample's phase lifetime. This phase difference between the fluorescence phase due to the sample and from the instrument, when referenced to the instrument without any sample, will give the sample's phase lifetime according to Equation S2 below. After an image of the laser response, the long-pass filter is put back in and a phase is recorded for each pixel. There is sufficient leak-through of the 532nm laser light through the dichroic that only the long-pass filter right before the PMT need be removed to measure the instrument response. Several laser scans were taken at the beginning, middle, and end of an imaging session to verify that lifetime values were fairly consistent. The phase lag due to the sample is the phase recorded from the sample after subtracting the laser phase. Usually this is done by subtracting an average of points over a smooth laser image from the actual cell image. The fluorescence lifetime at each pixel was determined from the phase lag at each pixel according to the simple relation:

$$\tau_\varphi = \omega^{-1}\tan(\Delta\varphi) \qquad \textbf{(Equation S2)}$$

where **ω** is the angular modulation frequency and **Δφ** is the experimentally observed phase lag. The sample was scanned with a piezo-electronic nanometric sample scanner (Physik Instrumente, PI nano), although the viscosity and chemical micro-environment is measured with a spatial resolution limited by that of the diffraction-limited optics (~300nm). All imaging and analysis was done on home-written software using LabView.

Fluorescence lifetime data of TMP-Cy3 in glycerol/water solutions of varying volume fraction from 0-100% were also taken on a single-photon counting fluorescence lifetime spectrometer (OB920, Edinburgh Analytical Instruments, U.K.) equipped with a PicoQuant 496nm pulsed LED diode as the excitation light source. The results were similar to what we obtained with the home-built FLIM microscope apparatus, for example, the measured fluorescence lifetime of TMP-Cy3 was the same for both (~0.3 ns).

## 3. Additional Spectroscopic Measurements on TMP-Cy3

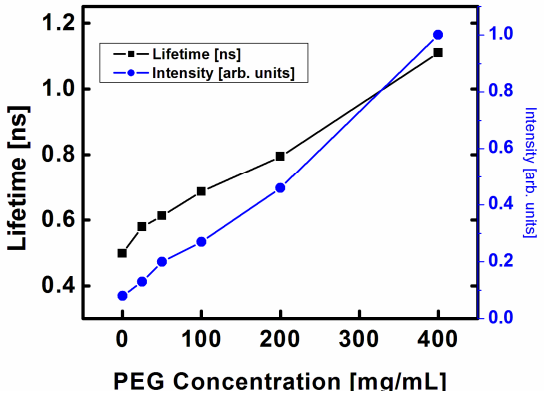


**Figure S5. Fluorescence lifetime and intensity of TMP-Cy3 as a function of PEG concentration.**

As a further test of the effect of viscosity and molecular crowding on the lifetime and intensity of Cy3, both the lifetime and intensity were measured in various concentration solutions of polyethylene glycol (PEG) from 0, 25, 50, 100, 200, to 400 mg/mL of PEG. An increase in both the lifetime and intensity were seen, with values approaching that of a 40-60% glycerol solution as the concentration was increased from 200 to 400 mg/mL.

As opposed to simple tests in glycerol and PEG solutions, using Cy3 to report on local cellular micro-viscosities requires further careful tests on solutions approximating the cellular environment. Two important concerns in the confocal intensity and FLIM mapping of intracellular viscosity are non-specific binding to cellular macromolecules (DNA, protein, lipid membranes, etc…) and the effect of other parameters such as polarity of the environment on the fluorescence intensity and lifetime of Cy3. Therefore, we performed systematic fluorescence intensity measurements in several solutions (DCM, ethanol, DMSO, dioxane, SDS and NaCl) and biomolecules (DNA and proteins). Solutions of 1μM TMP-Cy3 were prepared for all measurements and the absorption and fluorescence of Cy3 were recorded with a commercial plate reader (Tecan Infinite 200). Error was calculated by comparing the differences between several measurements on similar samples in the same run. All fluorescence intensities were normalized with respect to TMP-Cy3 in $H_2O$. Fluorescence intensity measurements can be

surrogates for lifetime measurements as they are affected by the same non-radiative decay mechanisms, although there are important differences as seen with the BSA lifetime data in Figure S11.

We tested the amphiphilic detergent Sodium Dodecyl Sulfate (SDS). SDS has an effect on the fluorescence intensity of TMP-Cy3 as observed by an increase in the fluorescence intensity by ~80% between pure $H_2O$ and a 10 mg/mL solution of SDS. Apparently there is a non-specific interaction between TMP-Cy3 and, presumably, the micelles formed by SDS. Interestingly, there is no significant change in the fluorescence intensity of TMP-Cy3 in going from a 10 mg/mL to a 20 mg/mL solution of SDS. The observed increase in TMP-Cy3 fluorescence intensity in solutions of SDS may help explain the non-specific binding of Cy3 to mitochondria and lipid membranes in our cellular measurements.

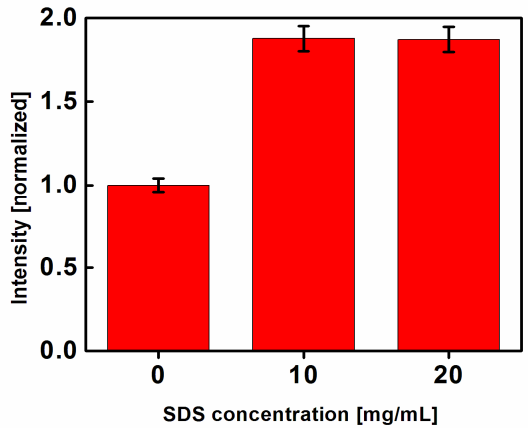


**Figure S6. There is a significant increase in the fluorescence intensity of a 1 µM TMP-Cy3 between pure $H_2O$ and 10 mg/mL of added SDS detergent, but not at higher concentration.**

We performed assays of the effect of ionic strength on TMP-Cy3 fluorescence in solution. As shown in Figure S7 below, there is a minimal effect on the fluorescence intensity of TMP-Cy3 with increasing concentration of NaCl from 0 M to a 1.0 M concentration solution of $H_2O$/NaCl.

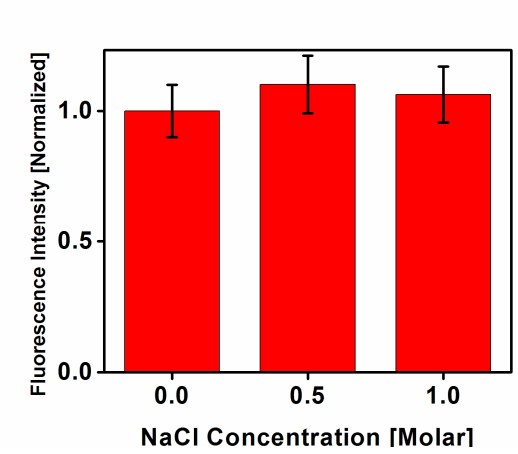


**Figure S7. There is a minimal effect of ionic concentration on the fluorescence of TMP-Cy3.**

We performed several assays of the effect of the presence of higher and higher concentrations of DNA in solution on the fluorescence intensity of TMP-Cy3 in solution. As shown in Figure S8 below, there is no significant change in the fluorescence intensity upon addition of increasing amounts of DNA.

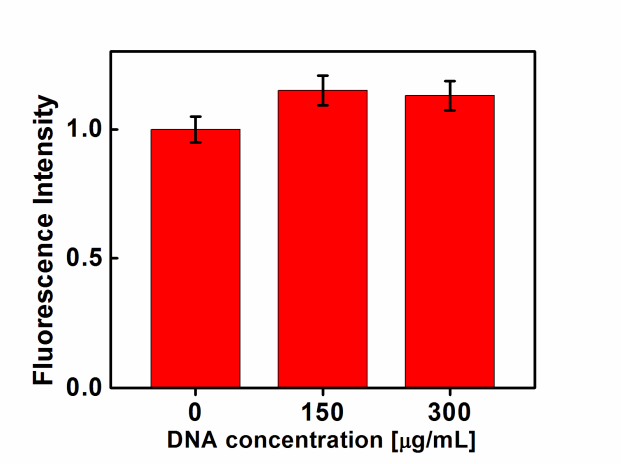


**Figure S8. Fluorescence intensity of 1 µM TMP-Cy3 as a function of DNA (plasmid DNA encoding PMLS-eDHFR was used) concentration, normalized with respect to 1 µM TMP-Cy3 in $H_2O$.**

Although not present in the cell, we tested the fluorescence of TMP-Cy3 in a variety of solvents as follows: DMSO, Ethanol, DCM, and in an assay of Dioxane/H2O with varying volume percentages. In pure solvents, there is a notable change in the fluorescence intensity of TMP-Cy3, as shown in Figure S9.

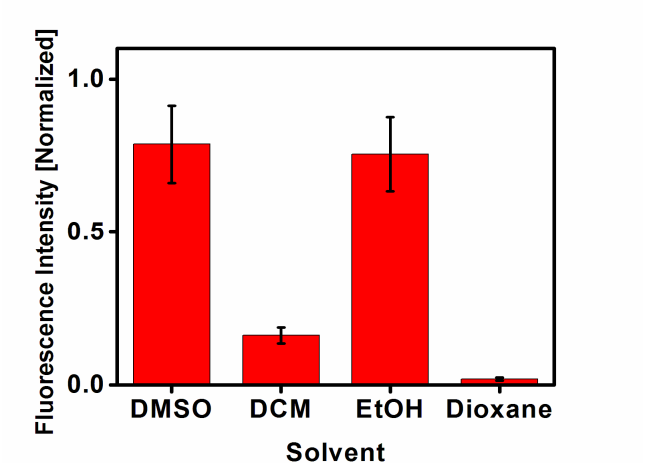


**Figure S9. The solvent does affect the fluorescence intensity of TMP-Cy3, when compared to a pure $H_2O$ solution (normalized to 1.0).**

In solutions of Dioxane/$H_2O$ from 0% to 75% volume/volume of Dioxane, there is an increase in the fluorescence intensity in going from 0% to 50% dioxane by a factor of about 30% (Figure S9). However, in a pure Dioxane solution, the fluorescence intensity drops considerably, to

<10% of that in pure $H_2O$ (see Fig. S9). Error bars for all charts were calculated from the error between several identical measurements.

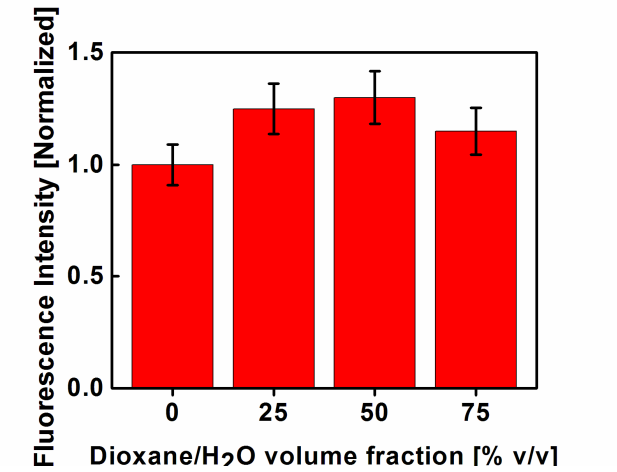


**Figure S10. There is an increase in the fluorescence intensity of TMP-Cy3 with increasing dioxane percentage, by about 30% from 0% to 50%, followed by a slight decrease.**

We also had to assess the effect of typical chemical species that can be found in the intracellular environment on the fluorescence lifetime, since we used the fluorescence lifetime for viscosity measurements. Additional experiments were performed in solutions of NaCl, SDS (where there was a significant change in the fluorescence intensity, but not the lifetime), the protein BSA, and other chemical species. No significant change was seen in the fluorescence lifetime upon changing the concentration of a series of some of the types of chemical species that would be encountered in the cell (ions, lipid domains, protein). A commercial lifetime fluorometer (OB920, Edinburgh Analytical Instruments, U.K.) with a PicoQuant 496nm pulsed LED diode as the excitation source was also used for the solution lifetime measurements, and we obtained values comparable to our homebuilt FLIM apparatus. Each run took 20 minutes – which would not be compatible with biological imaging. We do note that there was evidence of multi-exponential behavior in the BSA lifetimes, with one component around 50% at ~1.5ns and another component around ~50% closer to 3ns. Multi-exponential components can also be resolved with frequency domain FLIM, but would require an Electro-Optic Modulator and a larger frequency sweep or more expensive time-correlated single-photon counting (TCSPC) electronics. The data for water, NaCl, SDS, and BSA are shown below in Table 1.

| |
|---|
| H2O: 0.30 ns |
| SDS 10 mg/ml : 0.51 ns |
| SDS 20 mg/ml : 0.50 ns |
| NaCl 0.5 M : 0.33 ns |
| NaCl 1.0 M: 0.34 ns |
| BSA 50 mg/ml : 2.22 ns (if double-exponential: 35% 1.49 ns and 65% 2.76 ns ) |
| BSA 100 mg/ml : 2.23 ns (if fit in double-exponential: 49% 1.62 ns and 51% 3.00 ns) |
| BSA 200 mg/ml : 2.18 ns (if fit in double-exponential: 47% 1.55 ns and 53% 2.93 ns) |

**Table 1.** **Raw lifetime data from a commercial lifetime fluorometer for water, SDS, NaCl, and BSA solutions of TMP-Cy3. There is an observed high lifetime for concentrated solutions of BSA, but lifetimes are more constant than intensities.**

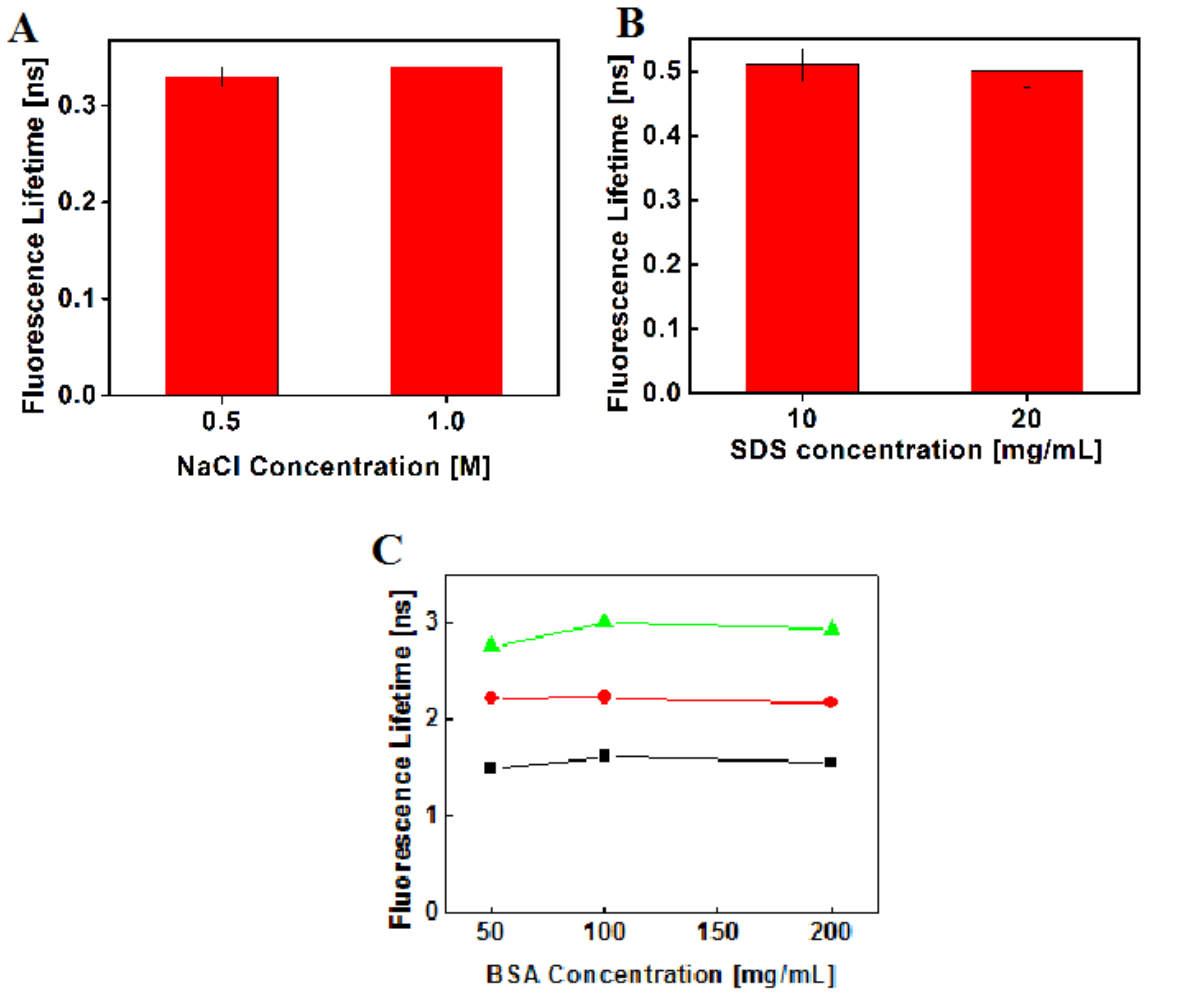


**Figure S11. There is no observable change in the fluorescence lifetime with increasing NaCl from 0.5 to 1M (A) or SDS concentration from 10 to 20 mg/mL (B). BSA lifetimes are fairly constant, although high, and there is the possibility of multi-exponential behavior with a lower-lifetime component (black), average (red), and high-lifetime component (green) (C).**

With BSA, there is an increasing fluorescence lifetime with increasing BSA concentration; this indicates that the fluorescence lifetime is indeed reporting on local viscosity as increasing protein concentration can dramatically increase viscosity. The fluorescence lifetime can also reveal information about protein environments that is obscured or less obvious from the fluorescence intensity alone. Overall, the fluorescence lifetime data is more constant than the intensity data but there is a demonstrable protein effect on lifetimes not seen in the fluorescence intensity data alone.

## REFERENCES

1. S. S. Gallagher, C. Jing, D. S. Peterka, M. Konate, R. Wombacher, L. J. Kaufman, R. Yuste, V. W. Cornish, *Chembiochem.*, 2010, **11,** 782-784.

2. R. Wombacher, M. Heidbreder, S. van de Linde, M. P. Sheetz, M. Heilemann, V. W. Cornish, M. Sauer *Nat. Methods*, 2010, **7,** 717-721.

3. L. W. Miller, Y. Cai, M. P. Sheetz, V. Cornish, *Nat. Methods* 2005**, 2,** 255-257.